

# A model investigation of turbulence-driven pressure-pumping effects on the rate of diffusion of CO<sub>2</sub>, N<sub>2</sub>O, and CH<sub>4</sub> through layered snowpacks

W. J. Massman and R. A. Sommerfeld

Rocky Mountain Station, USDA Forest Service, Fort Collins, Colorado

A. R. Mosier

USDA Agricultural Research Service, Fort Collins, Colorado

K. F. Zeller, T. J. Hehn, and S. G. Rochelle

Rocky Mountain Station, USDA Forest Service, Fort Collins, Colorado

This file was created by scanning the printed publication.  
Errors identified by the software have been corrected;  
however, some errors may remain.

**Abstract.** Pressure pumping at the Earth's surface is caused by short-period atmospheric turbulence, longer-period barometric changes, and quasi-static pressure fields induced by wind blowing across irregular topography. These naturally occurring atmospheric pressure variations induce periodic fluctuations in airflow through snowpacks, soils, and any other porous media at the Earth's surface. Consequently, the uptake or release of trace gases from soils and snowpacks is a combination of molecular diffusion and advection forced by pressure pumping. Using model-estimated fluxes, this study attempts to quantify the influence that turbulent pressure fluctuations with periods between 0.1 and 1000 s can have on the rate of exchange of CO<sub>2</sub>, N<sub>2</sub>O, and CH<sub>4</sub> through a seasonal snowpack. Data for this study were collected at a forested subalpine meadow site in the Rocky Mountains of southern Wyoming, during February 1995 when the snowpack was distinctly layered and approximately 1.4 m deep. The data include mole fraction of CO<sub>2</sub>, N<sub>2</sub>O, and CH<sub>4</sub> just above and at the base of the snowpack, several profiles of CO<sub>2</sub>, N<sub>2</sub>O, and CH<sub>4</sub> mole fraction in the top 1 m of the snowpack, and a profile of snowpack density and tortuosity. Turbulent atmospheric pressure-pumping fluctuations, sampled at approximately 11 Hz for several hours, were obtained with a fast response differential pressure sensor. A one-dimensional steady state diffusion model and one- and three-dimensional time-dependent pressure-pumping models are used to estimate the gas fluxes through the snowpack. Boundary conditions are provided by grab samples just above the snowpack and at the soil/snow interface. The pressure-pumping models are driven by the observed pressure fluctuations, and all models include the observed layering of the snowpack. As with previous studies the present results indicate that the effects of pressure pumping are diminished with increasingly strong gradients. Furthermore, we conclude that unless pressure pumping influences the gas concentrations at the boundaries of the snowpack, it appears unlikely that it can significantly impact the rate of gaseous diffusion through the snowpack. Even two- and three-dimensional effects, which can have a significant short-term impact on the fluxes and concentration profiles, are nearly eliminated when averaged over a period of hours. It is also suggested that vertical layering is important for three-dimensional pressure-pumping studies and that the time-dependent temperature term, which is traditionally ignored when modeling dynamic pressure variations, may in fact be dominant in some situations and probably should be incorporated in future modeling studies of pressure pumping.

## 1. Introduction

Because global increases in CO<sub>2</sub>, N<sub>2</sub>O, and CH<sub>4</sub> may significantly affect the global climate, stratospheric ozone, and global atmospheric chemistry [Houghton *et al.*, 1990; Turco, 1992], much effort has been directed toward identifying the processes and interactions that influence the soil's uptake and release of these gases. Even during the wintertime, these gases

can be produced or consumed by snow-covered soils [Sommerfeld *et al.*, 1993; Zimov *et al.*, 1993]. By causing air to move through snowpacks, pressure pumping is a potentially important process for the exchange of heat [Colbeck, 1989; Albert and Hardy, 1995], aerosols [Gjessing, 1977; Cunningham and Waddington, 1993], and trace gases [Massman *et al.*, 1995] between the atmosphere and the snow-covered surface. In general, atmospheric pressure pumping at the Earth's surface is ubiquitous in time, ranging on a scale of days [Massmann and Farrier, 1992] to fractions of a second [Clarke *et al.*, 1987], and ubiquitous with location [e.g., Sorrells *et al.*, 1971; Bovsheverov *et al.*,

This paper is not subject to U.S. copyright. Published in 1997 by the American Geophysical Union.

Paper number 97JD00844.

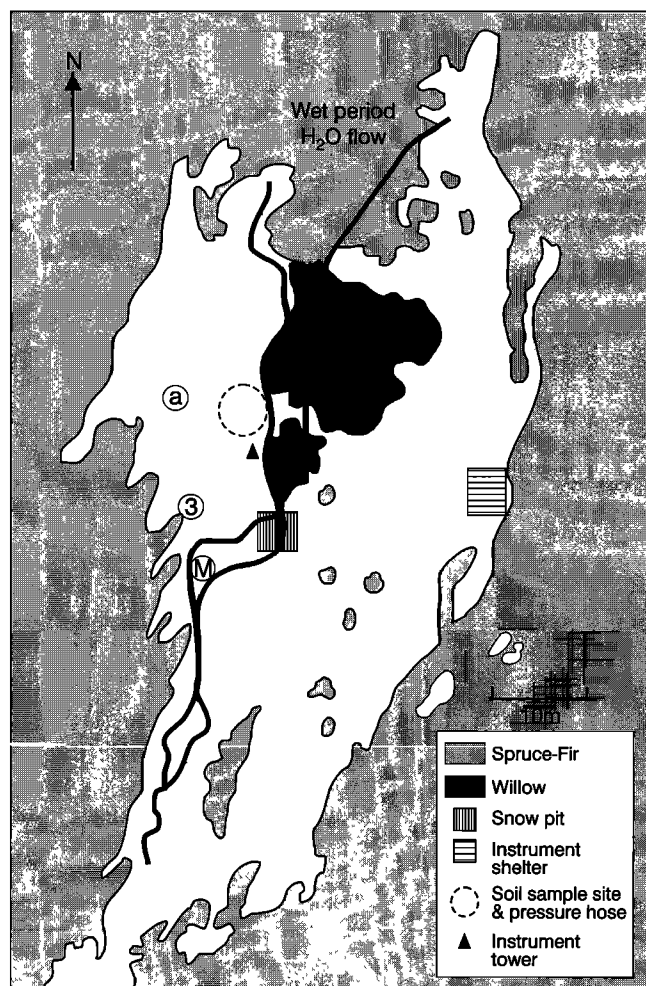


**Figure 1.** Drawing from an aerial photograph and field notes of the subalpine wet meadow pressure-pumping experiment site, located within the Glacier Lakes Ecosystem Experiments Site (GLEES) in the Snowy Range of the Rocky Mountains in southern Wyoming. The meadow is within a spruce-fir forest at an elevation of 3186 m. Trace gas samples were taken at the three locations marked “a,” “3,” and “M” during late February 1995 when the snow depth was 1.16 m (a), 1.57 m (3), and 1.68 m (M). The snow pit, pressure hose, and soil sample locations are also shown. Snowpack temperatures were obtained by a thermocouple array positioned near the tower site. The snow depth was 1.16 m at the snow pit site and 1.35 m at the thermocouple array. The dominant wind direction is from the west between 230° and 310°.

1973; Wilczak *et al.*, 1992]. For snowpacks, pressure pumping can be caused by pressure drag across surface topography in the direction of the wind [Colbeck, 1989], by atmospheric turbulence [Clarke and Waddington, 1991], and by low-frequency barometric changes [Massmann and Farrier, 1992]. Previous studies have also suggested that pressure drag across topography is likely to dominate either turbulent or barometric pressure pumping [Colbeck, 1989] and that pressure pumping by atmospheric turbulence is caused mostly by frequencies lower than about 0.1 Hz [Albert, 1993].

The purpose of the present study is to investigate the effects that high-frequency turbulent atmospheric pressure fluctuations with periods between 0.1 and 1000 s can have upon the fluxes of CO<sub>2</sub>, N<sub>2</sub>O, and CH<sub>4</sub> into and out of snowpacks. This

study extends the results of Massman *et al.* [1995] to include (1) N<sub>2</sub>O and CH<sub>4</sub>, (2) a derivation of the advective-diffusive equations that form the basis of the pressure pumping model in a manner that is consistent with Graham’s law [e.g., Farr, 1993], and (3) an exploration of some of the differences between one-dimensional (1-D) and three-dimensional (3-D) models of pressure pumping in snowpacks.

## 2. Materials and Methods

### 2.1. Site Description

Data for this study were obtained between February 22 and 24, 1995, at a subalpine wet meadow site (elevation 3186 m) within the larger Glacier Lakes Ecosystem Experiments Site (GLEES) (41°20’N, 106°20’W), located in the Rocky Mountains of southern Wyoming about 70 km west of Laramie, Wyoming. Musselman [1993] and Massman *et al.* [1995] give a more detailed description of the geology, soils, vegetation, and topography of GLEES. The approximately 0.5 ha meadow is surrounded by subalpine forest composed of trees between 15 and 20 m in height. Although the average winter wind speed at the GLEES site is about 10 m s<sup>-1</sup>, the sheltering effect of the trees reduce the mean wind speeds within the meadow to between 1 and 4 m s<sup>-1</sup>. Nevertheless, blowing and drifting is common, so snow depth can vary significantly within the meadow. However, during the time of the experiment the drifting was such that the axis of the major wind-created topographical features was approximately perpendicular to the wind direction. Figure 1 is a schematic of the meadow site and the experimental setup, and provides some detail on the snow depth around the meadow.

### 2.2. Data

**2.2.1. Pressure measurements.** Turbulent pressure fluctuations were archived after sampling almost continuously at 11 Hz on two separate occasions. The first (or phase I) was from 2200 LT on February 21 through 0600 LT on February 24, and the second (or phase II) was from 2200 LT on March 7 through 0300 LT on March 8, 1995. The pressure data collected during the later period is used for model sensitivity analyses. These data were obtained with a differential pressure transducer [Cook and Bedard, 1971] attached to two lengths of a laser-perforated hose (a common garden hose known as a “soaker” hose) attached in series. The hoses were then laid over 10–15 m<sup>2</sup> of snow surface. The effects of a 100-s high-pass filter, designed to be part of the instrument, were removed using numerical techniques before using the pressure data to drive the model. Any residual effects associated with weak temperature sensitivity of the instrument or standing pressure waves induced by variations in the snow depth are removed from the pressure data by eliminating the mean offset in pressure for every half hour of data.

Nevertheless, because the hose averages the pressure signal over a finite area, sampling turbulent pressure fluctuations with a hose attenuates some of the high-frequency components present in the data [Bovsheverov *et al.*, 1973]. On the other hand, these high-frequency components (0.1–10 Hz) may not be too important for pressure pumping [Albert, 1993]. The effects of this loss will be discussed in a later section by comparing spectra of the pressure data obtained with the soaker hose to pressure data obtained with the “Quad-Disc” [Nishiyama and Bedard, 1991], which is designed to sample ambient atmospheric pressure fluctuations at a single point. The

“Quad-Disc” data were obtained in late September and early October 1993 and will also be used for the sensitivity analyses.

**2.2.2. Snowpack and soil data.** Half-hourly averaged snowpack temperatures were obtained with a vertical array of 30-gauge copper-constantan thermocouples deployed every 20 cm within the snowpack starting at the soil surface. This array, suspended from a piece of nylon dental floss, had been installed during the previous fall, and the snow was allowed to build up around it. These temperatures are input directly into the model as estimates of snowpack temperature and to model the temperature effects on the dynamic viscosity of air and the diffusivity of CO<sub>2</sub>, N<sub>2</sub>O, and CH<sub>4</sub> in air.

Ambient atmospheric concentration approximately 1 cm above the snow surface and profiles of snowpack concentration for each of the three trace gases examined in this study were obtained at three locations within the meadow site by grab samples. All samples were taken using (1/16 inch OD) Teflon tubing and/or 20-mL nylon syringes fitted with nylon stopcocks [Sommerfeld *et al.*, 1993]. All gases were sampled 3 times on February 23 at 5, 10, 30, 50, and 100 cm below the snow surface and at the base of the snowpack. In addition, profiles of CO<sub>2</sub> and CH<sub>4</sub> were also sampled once on both February 22 and 24. All gas samples were analyzed by gas chromatography as soon after they were drawn as possible [Sommerfeld *et al.*, 1993]. They were then screened to remove obvious outliers and averaged to produce, at each of the three locations, a single concentration profile for each of the three gases studied. Snow depth varied between 1.16 and 1.68 m at the three sampling locations, and the farthest locations were separated by 15–20 m (Figure 1). Data from these three locations are used to indicate the spatial variation of the fluxes.

Profiles of snow density and texture were obtained on February 24 from a snow pit (Figure 1). The snow depth at the snow pit location was 1.16 m. In addition, we also preserved snow samples in dimethyl phthalate [Perla, 1982] for later analysis of snowpack tortuosity profiles. Similar to Winston *et al.* [1995], we cut, polished, and prepared the sections in the cold room for imaging. After classifying the digitized images into air and ice phases, we averaged 10 streamlines constructed through the pore space to evaluate tortuosity. Although tortuosity is a property of a three-dimensional matrix, we believe that, providing the snowpack is not extremely anisotropic, this method can be used to accurately estimate tortuosity.

Two soil cores were taken during fall 1994 at the meadow site (Figure 1) and analyzed for profiles of bulk density, texture, and saturated hydraulic conductivity. Soil air permeability was then estimated from hydraulic conductivity profiles.

## 2.3. Model Formulations

**2.3.1. Atmospheric pressure pumping (1-D) and general considerations.** The model equations used in this study are based on the advective-diffusive equations used to describe the flow of a gas through a porous medium. The 1-D version of these equations is given below, and the 3-D version is developed in the next section.

$$v = -\frac{k}{\mu} \frac{\partial p}{\partial z} \quad (1)$$

$$\eta c \frac{\partial \chi}{\partial t} = -c \frac{\partial(\chi v)}{\partial z} + \frac{\partial}{\partial z} \left( c \eta \tau D \frac{\partial \chi}{\partial z} \right) \quad (2)$$

$$\eta \frac{\partial c}{\partial t} = -\frac{\partial(c v)}{\partial z} \quad (3)$$

Here  $t$  is time,  $z$  is depth measured from the snow surface,  $v$  is advective velocity,  $k$  is the permeability of the medium,  $\mu$  is the dynamic viscosity of air,  $p$  is the fluctuating component of the pressure,  $\eta$  is the porosity of the medium,  $\chi$  is the mole fraction of gas moving through the medium (ppmv or ppbv),  $c$  is the total molar concentration of air and trace gas,  $\tau$  is tortuosity of the medium (here we define tortuosity such that  $0 < \tau \leq 1$ ), and  $D$  is the binary diffusivity of a given gas in air. In general, because snowpacks are layered,  $k$ ,  $\eta$  and  $\tau$  are all considered as functions of depth; on the other hand, however, because the duration of this experiment is only a few hours, we assume that  $k$ ,  $\eta$ , and  $\tau$  are not functions of time.

Equation (1) is Darcy’s law; (2) is the conservation of mass for CO<sub>2</sub>, N<sub>2</sub>O, or CH<sub>4</sub>; and (3) is the conservation of mass for air. The more familiar form of (3) is usually expressed in terms of  $p$ , as will be discussed below. Equations (2) and (3) are approximations of the more exact transport equations used to describe the advective-diffusive transport of a binary gas through a porous medium. The exact equations are given in the appendix along with a discussion of the approximations made when deriving (2) and (3). In this study the concentrations of CO<sub>2</sub>, N<sub>2</sub>O, and CH<sub>4</sub> are so dilute that we treat each gas independently of the other two. Darcy’s law also assumes laminar flow within the snowpack pore space. In addition to this, (1)–(3) do not include Knudsen effects, gravitational settling, or viscous flow [e.g., Farr, 1993], all of which are expected to be unimportant for this study.

Substituting the ideal gas law,  $c = P/RT$ , and (1) into (3) yields the following equation for  $p$ :

$$\frac{\partial p}{\partial t} = \frac{TP_0}{\eta} \frac{\partial}{\partial z} \left( \frac{k}{T\mu} \frac{\partial p}{\partial z} \right) + \frac{P_0}{T} \frac{\partial T}{\partial t} \quad (4)$$

where  $R$  is the universal gas constant,  $T$  is temperature (in kelvins),  $P_0$  is the nonvarying or time-independent ambient background pressure ( $P_0 \approx 70$  kPa during the experiment), and  $P$  is the total ambient pressure (i.e.,  $P = P_0 + p$ ; in general,  $P_0 \gg p$  can be assumed). Except for the temperature gradient and time-varying temperature term, (4) is the usual form of the one-dimensional dynamic pressure equation [e.g., Massmann and Farrier, 1992; Clarke *et al.*, 1987]. For the present we do not include the term  $(P_0/T)(\partial T/\partial t)$  in the model, although we do include it in the sensitivity analyses. We defer further consideration of this term until the end of this section. Consequently, the 1-D version of the snowpack pressure used in this study is

$$\frac{\partial p}{\partial t} = \frac{TP_0}{\eta} \frac{\partial}{\partial z} \left( \frac{k}{T\mu} \frac{\partial p}{\partial z} \right) \quad (5)$$

This formulation includes the temperature gradient effects because the measured snowpack and soil temperatures are input directly into the model.

Snow permeability, dynamic viscosity, and diffusivity are modeled as follows:

$$k = k_0 \exp(-9.57\rho_{\text{snow}}) \quad (6)$$

$$\mu = \mu_0 \left( \frac{T_{23} + T_{120}}{T + T_{120}} \right) \left( \frac{T}{T_{23}} \right)^{3/2} \quad (7)$$

$$D = D(0) \left( \frac{P_{00}}{P_0} \right) \left( \frac{T}{T_0} \right)^{1.81} \quad (8)$$

where  $k_0 = 1.096 \times 10^{-8}$  m<sup>2</sup>,  $\rho_{\text{snow}}$  is the measured snowpack density in megagrams per cubic meter or grams per cubic

centimeter (we restate here that  $\rho_{\text{snow}}$  can vary with depth within the snowpack),  $\mu_0 = 1.8532 \times 10^{-5} \text{ kg m}^{-1} \text{ s}^{-1}$  (for computational purposes, note that  $1 \text{ kg m}^{-1} \text{ s}^{-1} = 1 \text{ Pa s}$ ),  $P_{00}$  is sea level pressure = 101.3 kPa,  $D(0)$  is the binary diffusion coefficient of the trace gas in air at  $0^\circ\text{C}$ ,  $T_0 = 273.15^\circ\text{K}$ ,  $T_{23} = T_0 + 23^\circ\text{K}$ , and  $T_{120} = 120^\circ\text{K}$ . Here (6) is taken from *Sommerfeld and Rocchio* [1993] and (7) and (8) are from *List* [1971]. The diffusivity  $D(0)$  of  $\text{CO}_2$  in air is taken to be  $0.139 \times 10^{-4} \text{ m}^2 \text{ s}^{-1}$  [Hodgman and Lange, 1925], and  $D(0)$  for methane is taken as  $0.196 \times 10^{-4} \text{ m}^2 \text{ s}^{-1}$  [Roberts, 1972]. Measurements of the diffusivity of  $\text{N}_2\text{O}$  in air suggest that  $D(0)$  for  $\text{N}_2\text{O}$  differs by less than 3% from  $D(0)$  for  $\text{CO}_2$  [Pritchard and Currie, 1982], and estimates of  $D(0)$  for  $\text{N}_2\text{O}$  from the Chapman-Enskog kinetic theory of gases [Bird et al., 1960; Bretsznajder, 1971] suggest that the difference is less than 2%. For simplicity we assume that  $D(0)$  for  $\text{N}_2\text{O}$  and  $\text{CO}_2$  are the same.

The 1-D pressure-pumping model equations (1), (2), and (5) are solved numerically by finite difference methods to produce half-hourly flux estimates on February 22, 1995, between 0530 and 2030 (MST). We use the backwards implicit method for the time differencing and a second-order mass conserving scheme for the spatial differencing. The spatial grid has a uniform spacing of 0.001 m, and the time step, determined by the sampling rate of the differential pressure sensor, is 0.091 s. The half-hourly flux is the average of the instantaneous fluxes computed at each time step. Equation (2) is initialized assuming a linear profile in  $\chi$  and (5) is initialized assuming a weakly decreasing pressure amplitude. The first half hour of any simulation is not used in the subsequent analysis. The boundary conditions for (2) are estimated from the several grab samples taken within 0.01 m of the snowpack surface and from the soil-snowpack interface. For any given half-hourly flux estimate these boundary conditions are assumed to be constant. Nevertheless, like pressure, ambient atmospheric concentrations of  $\text{CO}_2$  and other trace gases also display high-frequency turbulent fluctuations. Consequently, we use an open path  $\text{CO}_2$  sensor [Auble and Meyers, 1992], mounted about 1.3 m above the snow surface, to investigate possible influences these fluctuations could have on the upper boundary condition and on the corresponding fluxes. The results of this investigation are included in the sensitivity analysis. The upper boundary condition on (5) is supplied by the high-frequency pressure data. The lower boundary condition for (5) is  $v = 0$  at the level of the bedrock, which is estimated from the soil samples to be 0.69 m below the soil surface. The bedrock is assumed to be impermeable.

The portion of the model domain that describes the pressure pumping includes both snowpack and soil. Because the soil is porous, neither the pressure fluctuation  $p$  nor the induced advective velocity  $v$  is likely to vanish at the soil-snowpack interface. Consequently, we include a layered soil in the formulation of the lower boundary condition for (5). On the other hand, the domain of the trace gas component of the model, equation (2), includes only the snowpack. Much of the evidence we have to date suggests that it is not necessary to explicitly model the evolution or uptake and transport of  $\text{CO}_2$ ,  $\text{N}_2\text{O}$ , or  $\text{CH}_4$  within the soil because the soil uptake and release of these gases are sufficiently constant with time to be ignored during the few hours of the experiment.

We do not directly include  $(P_0/T)(\partial T/\partial t)$  in the present study because to do so requires modeling the movement of water vapor through the snowpack [Albert and McGilvary,

1992] which would make the model more complex than seems warranted at this time. Nevertheless, the sensitivity analyses include a diel cycle of snowpack temperature parameterized using  $(P_0/T)(\partial T/\partial t)$  and an order of magnitude evaluation of  $(P_0/T)(\partial T/\partial t)$  relative to  $\partial p/\partial t$  for high-frequency turbulent fluctuations in  $p$  and  $T$ . The purpose of the order of magnitude evaluation is to determine quantitatively whether ignoring the time-dependent temperature term is justifiable or not. For simulating the snowpack's daily temperature cycle we use an approximation to the following model by *van Wijk and de Vries* [1963].

$$\frac{P_0}{T} \frac{\partial T}{\partial t} = \pm \frac{P_0}{T} \omega \Delta T \exp\left(-\frac{z}{\delta}\right) \cos\left(\omega t - \frac{z}{\delta}\right) \quad (9)$$

where  $\omega$  is the frequency of the daily cycle ( $= 7.272 \times 10^{-5} \text{ s}^{-1}$ ),  $\Delta T$  is the amplitude of the daily cycle ( $= 10^\circ\text{C}$ ), and  $\delta$  is the damping depth [van Wijk and de Vries, 1963] of the snowpack ( $= \sqrt{2\lambda/\omega(1-\eta)\rho_i C_i}$ ). Here  $\lambda$  is thermal conductivity of ice,  $\rho_i$  is the density of ice, and  $C_i$  is the apparent specific heat capacity of ice [Mellor, 1977]. For the sensitivity analysis we assume that  $\omega t$  can be ignored for any given half hour, that the snowpack  $\delta$  is 0.2 m [from Mellor, 1977], that  $P_0 = 70 \text{ kPa}$ , and that  $T = 268^\circ\text{K}$ . We compute the model fluxes twice by varying the sign of the right-hand side of (9).

**2.3.2. Atmospheric pressure pumping (3-D).** To evaluate possible two- and three-dimensional effects, we generalize the 1-D model in a simple manner. In general, because observed vertical gradients of the trace gases are 10 to 100 times greater than the observed horizontal gradients, we expect that the changes in the vertical fluxes due to higher-dimensional effects will be dominated by horizontal variations in the pressure field not by horizontal variations in the concentrations or snowpack physical properties. Consequently, ignoring the horizontal gradients in  $T$ ,  $\mu$ ,  $k$ , and  $\chi$ , (2) and (5) can be expressed in three dimensions as follows:

$$\eta c \frac{\partial \chi}{\partial t} = -c \frac{\partial(\chi v)}{\partial z} + \frac{\partial}{\partial z} \left( c \eta \tau D \frac{\partial \chi}{\partial z} \right) + c \chi \frac{k}{\mu} (\nabla_h^2 p) \quad (10)$$

$$\frac{\partial p}{\partial t} = \frac{TP_0}{\eta} \frac{\partial}{\partial z} \left( \frac{k}{T\mu} \frac{\partial p}{\partial z} \right) + \frac{P_0 k}{\eta \mu} (\nabla_h^2 p) \quad (11)$$

where  $\nabla_h$  is the horizontal gradient operator. For the purposes of this study, (10) is the 3-D analog to (2), and (11) is the 3-D analog to (5). These two equations can be further simplified by using spectral methods to describe the horizontal pressure field, i.e., by assuming that the horizontal pressure field varies (in Cartesian coordinates) as  $\exp(ik_x x + ik_y y)$ , where  $x$  and  $y$  are the horizontal directions,  $k_x$  and  $k_y$  are the horizontal wave numbers, and  $i$  is  $\sqrt{-1}$ . Here  $k_x = 2\pi/\lambda_x$  and  $\lambda_x$  is the horizontal wavelength of the surface pressure perturbation in the  $x$  direction;  $k_y$  is similarly defined in the  $y$  direction. Denoting  $k_h$  as  $(k_x^2 + k_y^2)^{1/2}$  and  $\lambda_h$  as  $(\lambda_x^2 + \lambda_y^2)^{1/2}$ , then  $(\nabla_h^2 p)$  can be expressed as  $-k_h^2 p$ . Now using observed values for  $P_0$ ,  $k$ ,  $\eta$ , and  $\mu$  and estimating (somewhat arbitrarily) that  $\lambda_h \approx 5\text{--}10 \text{ m}$  suggests that  $(c\chi k/\mu)(\nabla_h^2 p) \approx -5 \times 10^{-5} c\chi p$  and  $(P_0 k/\eta\mu)(\nabla_h^2 p) \approx -5p$ . We do not include the vertical variations in snow permeability ( $k_{\text{snow}}$ ),  $\eta$ , or  $\mu$  in the horizontal terms because we cannot be very precise about the value assigned to  $\lambda_h$ , therefore that level of detail about  $k_{\text{snow}}$ ,  $\eta$ , or  $\mu$  is unnecessary. Nevertheless, the foregoing analysis demonstrates that assessing the influences of two- and three-dimensional effects can be accomplished relatively simply. The

results of the investigations with the 3-D model are included as part of the sensitivity analyses.

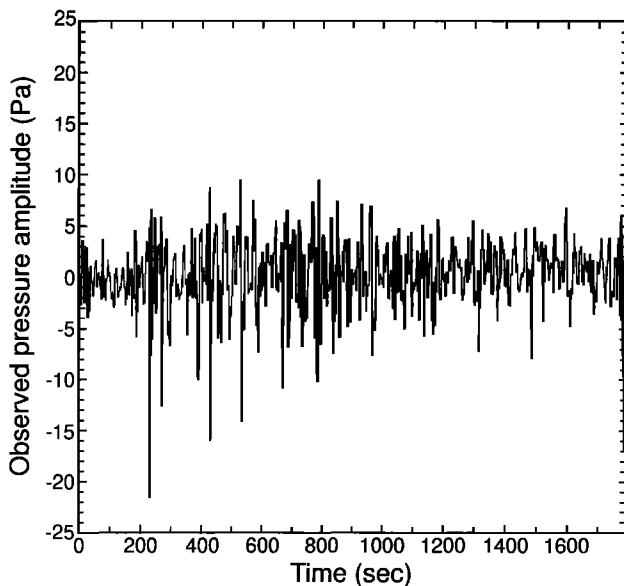
**2.3.3. Diffusion only.** The diffusion-only model is the same as (2) except that we assume conditions are steady state ( $\partial\chi/\partial t = 0$ ) and nonadvective ( $v = 0$ ). The spatial resolution, the boundary conditions, and the layering of the snowpack are all the same as with the pressure-pumping model. The diffusion-only model is integrated numerically by using a shooting method and a fourth-order Runge-Kutta approach, and the integration is repeated until the lower boundary condition is satisfied to within a small tolerance.

### 3. Results and Discussion

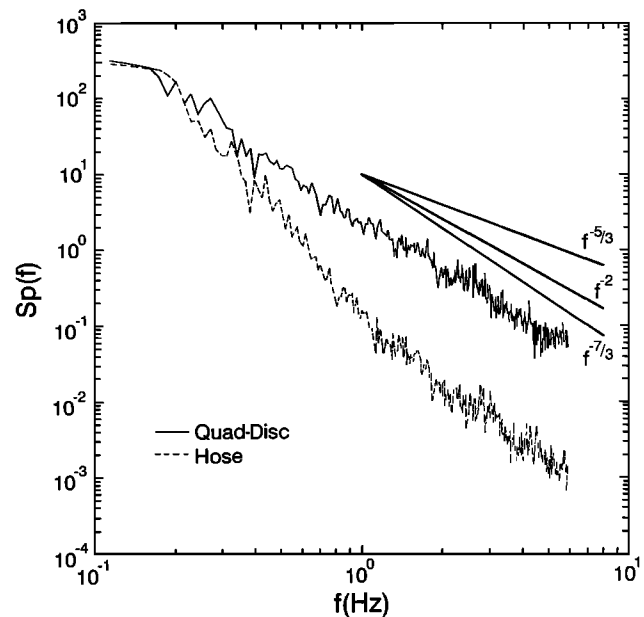
#### 3.1. Observed Pressure Fluctuations

Figure 2 is a representative sample of the pressure fluctuation data used to drive the model. This particular half hour of data was gathered at 0600 LT on February 22, 1995, and is quite typical of phase I pressure data. During this period the half-hourly root mean square (RMS) amplitude of the pressure fluctuations varied between about 0.8 and 3.6 Pa with excursions rarely exceeding 15 Pa. The wind speed, measured about 1.3 m above the snow surface with a three-axis sonic anemometer, varied between calm conditions and  $1 \text{ m s}^{-1}$  during phase I. During phase II the RMS amplitudes varied between 4.0 and 9.4 Pa with excursions frequently exceeding 25 Pa, while the wind speed varied between 1 and  $2 \text{ m s}^{-1}$ . Unlike the pressure data recorded during the winter of 1994 [Massman *et al.*, 1995], there is relatively little spectral power in the pressure fluctuations in the lower frequencies (corresponding to periods between about 10 and 30 min) during either of the 1995 data phases. As a result, we include as part of the model sensitivity analysis a discussion of potential influence that the lower-frequency components can have on the pressure-pumping fluxes.

Figure 3 compares the normalized power spectra when using the hose and when using the Quad-Disc. These spectra are



**Figure 2.** Half hour of observed pressure fluctuations with the hose deployed on the snow surface. Data were sampled at 11 Hz between 0530 and 0600 MST, February 22, 1995. At this time the wind speed was approximately  $0.8 \text{ m s}^{-1}$ .



**Figure 3.** Normalized spectra of observed pressure fluctuations when using the Quad-Disc and when using the hose. Attenuation of higher frequencies when using the hose is indicative of the effects of spatial averaging associated with the hose.

quite typical of all the observed half-hourly data, and like Bovsheverov *et al.* [1973], Figure 3 shows that spatial averaging attenuates the high-frequency portion of the spectra. However, unlike Bovsheverov *et al.* [1973] who suggest that spatial averaging attenuates frequencies greater than 0.01 Hz, our results suggest that the spatial filtering effects are largely confined to frequencies greater than about 0.1 Hz. This can be understood qualitatively by noting that the hose spatially averages turbulent eddies with horizontal dimensions of less than about 5 m, and at a wind speed of  $1 \text{ m s}^{-1}$  this corresponds (by Taylor's hypothesis) to an attenuation of frequencies above about 0.2 Hz. We also note here that the Quad-Disc pressure spectra, which should be more representative of atmospheric pressure fluctuations than the hose data, attenuate with frequency according to a  $-6/3$  to  $-7/3$  power law, similar to the observations discussed by Priestly [1965] but somewhat different than the  $-5/3$  power law suggested by Wilczak *et al.* [1992]. For the present study the Quad-Disc data were taken during unstable atmospheric conditions, whereas the hose data are obtained during neutral to slightly stable atmospheric conditions.

#### 3.2. Snowpack and Soil Characteristics

Table 1 lists the observed snow layers with their corresponding thicknesses, density, tortuosity, grain size, texture [Colbeck *et al.*, 1990], and temperature. The snow pit revealed a layered snowpack and was modeled as having six distinct layers. There was no evidence of ice lenses or gaps in the snow pack. Because the depth of the snowpack at the snow pit site was not the same as the depth at the gas sampling locations (Figure 1), we scaled the snowpack profiles to the observed depth at each of the sampling sites. The present snowpack data differ from the data used in the preceding study [Massman *et al.*, 1995] in two ways. First, Massman *et al.* [1995] did not measure tortuosity profiles; rather, they modeled snowpack tortuosity using a single value of 0.7 for all observed densities. Second, the snowpacks sam-

**Table 1.** Snowpack Structure From Snow Pit Observations (From Top of Snowpack Downward to Soil Surface)

Layer	Boundaries, cm	Density, gm cm <sup>-3</sup>	Tortuosity	Grain Size, mm	Texture*	Temperature, °C
1	0–26	0.241	0.89 ± 0.09	0.3	3C	–5.0
2	26–44	0.323	0.94 ± 0.06	0.3	3C	–4.5
3†	44–46	0.340	0.85 ± 0.08	0.5	6A	–4.5
4†	46–55	0.340	0.85 ± 0.08	0.3	3A	–4.5
5‡	55–69	0.347	0.85 ± 0.06	0.7	4A	–3.3
6‡	69–85	0.350	not available	1.0	4B	–3.3
7	85–99	0.280	0.75 ± 0.08	1.3	5A	–2.0
8	99–116	0.255	0.84 ± 0.04	3.0	5A/B	–1.6

\*In accordance with Colbeck *et al.* [1990].

†These two layers were combined for model simulations.

‡These two layers combined for model simulations, average density = 0.349 g cm<sup>-3</sup>.

pled during the earlier study (late February and early March 1994) showed more vertical structure, greater depth, and greater variation in density. All snowpack profiles were smoothed at the interface between each layer using a cubic spline to facilitate computations. Snowpack temperatures varied diurnally at all snowpack depths. Near the top of the snowpack they varied between about –9°C and –3°C, while near the bottom they varied between about –0.7°C and –0.2°C. The depth of the snowpack at the location of the thermocouple array was about 1.35 m. For computational simplicity and because temperature effects are relatively small, each snowpack layer was assigned a fixed value of temperature during all model runs. The influence that temperature gradient effects can have upon the fluxes is also explored in the section that discusses the results of the model sensitivity analysis.

The soil samples suggested that the soil could be modeled with five distinct layers and, as summarized by Table 2, each layer varies between 0.1 and 0.2 m in thickness with a total soil depth of 0.69 m. The soil layers were characterized by separate permeabilities varying between  $1.2 \times 10^{-12}$  and  $37 \times 10^{-12}$  m<sup>2</sup>. (Note that the values reported by Massman *et al.* [1995] are incorrect due to a typographical error.) Observed soil temperatures were nearly uniform with depth and constant with time and averaged about 0°C (slightly colder than 1°C reported in the previous study [Massman *et al.*, 1995]). For modeling purposes the soil is assumed to have a uniform soil temperature of 0°C. Because we are not directly modeling soil processes that consume or release CO<sub>2</sub>, N<sub>2</sub>O, or CH<sub>4</sub>, the exact soil temperatures are not particularly important to the modeled fluxes [Massman *et al.*, 1995].

Table 3 lists the observed trace gas mole fractions just above the snowpack (upper boundary condition) and at the base of the snowpack (lower boundary condition). Data entries listed as not available result from limitations in the number of bottles used to store the samples for transport to the laboratory for

analysis. Table 3 shows that the snowpack gradients are quite different for each of these three gases. The CO<sub>2</sub> concentration at the base of the snowpack is higher than ambient, whereas for CH<sub>4</sub> just the opposite is true. Furthermore, higher CO<sub>2</sub> or lower CH<sub>4</sub> concentrations correlate positively with greater snowpack depths. For N<sub>2</sub>O the upper and lower concentrations are nearly the same. These results are similar to the findings of Sommerfeld *et al.* [1993], who suggest that during winter CO<sub>2</sub> is generated within the soil, CH<sub>4</sub> is taken up within the soil, and N<sub>2</sub>O is very slowly released by the soil. Although there is some variation for all trace gas concentrations with position and time, only the lower boundary condition on CO<sub>2</sub> and CH<sub>4</sub> show any significant variation. At location “M” the variation of CO<sub>2</sub> is about ±10% (relative to the mean). For CH<sub>4</sub> the variation averages about ±20% for the three locations. The cause of these variations at fixed locations is not known but may be related to variation in the rate of soil production or consumption. All other boundary conditions show about a 3% variation, which is roughly comparable to the measurement uncertainty. Nevertheless, some of the observed variations in the ambient atmospheric concentrations (upper boundary condition) probably result from atmospheric turbulence. For example, the observed half-hourly RMS amplitude in CO<sub>2</sub> concentration measured with the open path CO<sub>2</sub> sensor at 1.3 m was typically between 1 and 5 ppmv, or about 1% to 2% of the mean CO<sub>2</sub> concentration. However, because no high-frequency trace gas measurements were made just above the snow surface, it is not possible to be more definite about the cause of the variations in the upper boundary condition. These variations in the

**Table 2.** Modeled Soil Structure (From Soil Surface Downward)

Layer	Boundaries, cm	Density, g cm <sup>-3</sup>	Permeability, 10 <sup>-12</sup> m <sup>2</sup>	Temperature, °C
1	0–10	0.9	1.2	0.0
2	10–20	0.9	15	0.0
3	20–31	1.0	4.7	0.0
4	31–51	0.9	37	0.0
5	51–69	0.9	14	0.0

**Table 3.** Average Ambient Mole Fraction and Observed Range of Variation of Trace Gases Within 1 cm of Top of Snowpack (Upper Boundary Condition) and at Soil-Snowpack Interface (Lower Boundary Condition)

Location (Figure 1)	CO <sub>2</sub> , ppmv	N <sub>2</sub> O, ppbv	CH <sub>4</sub> , ppmv
<i>Upper Boundary Condition</i>			
M	377 (368, 385)	319 (not available)	1.78 (1.72, 1.81)
3	380 (370, 390)	not available	1.77 (1.72, 1.85)
a	369 (361, 379)	315 (314, 316)	1.75 (1.72, 1.80)
<i>Lower Boundary Condition</i>			
M	3053 (2751, 3349)	326 (320, 332)	0.54 (0.44, 0.67)
3	2550 (2499, 2691)	not available	0.69 (0.57, 0.99)
a	2282 (not available)	329 (316, 342)	0.97 (0.91, 1.00)

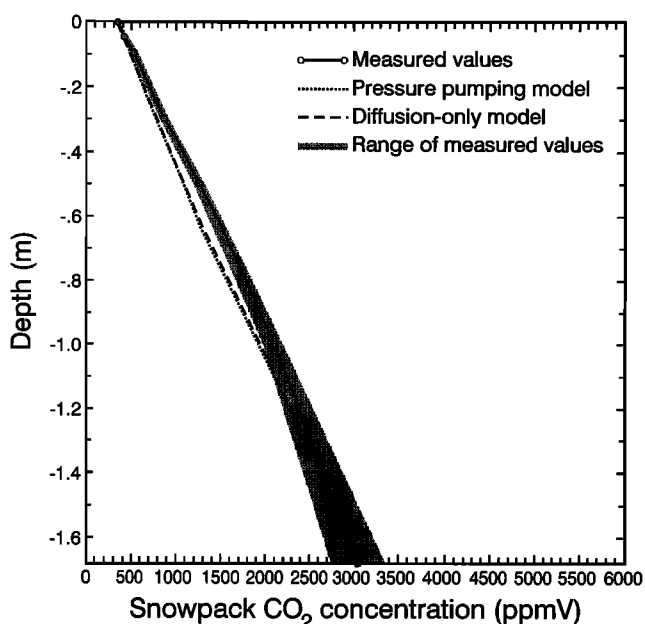


**Figure 4.** Modeled and observed snowpack CO<sub>2</sub> profiles during the experimental period February 22–24, 1995, at location “M” for the 1-D pressure-pumping model.

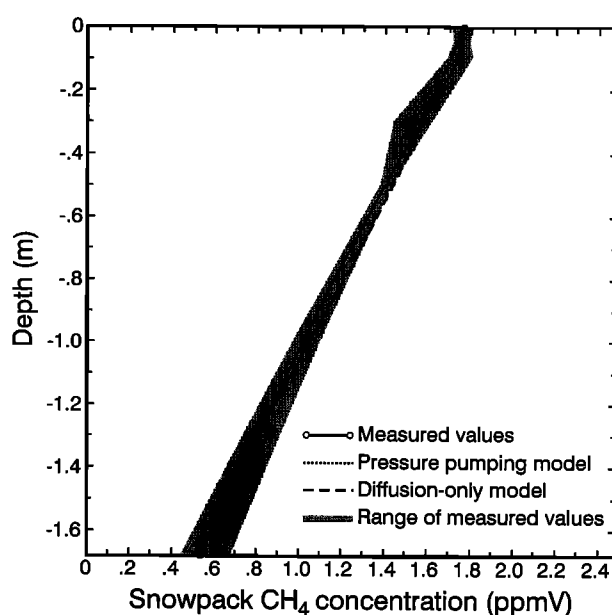


**Figure 6.** Modeled and observed snowpack CH<sub>4</sub> profiles during the experimental period February 22–24, 1995, at location “M” for the 1-D pressure-pumping model.

boundary conditions at a fixed location are eliminated by averaging all observations.

**3.3. Observed and Modeled Profiles of CO<sub>2</sub>, N<sub>2</sub>O, and CH<sub>4</sub> and Modeled Profiles of Pressure and Velocity**

Figure 4 shows the measured and modeled average snowpack CO<sub>2</sub> profiles for location M (Figure 1). The modeled CO<sub>2</sub> profile is taken at the end of an 18-hour simulation period. Figures 5 and 6 are the same as Figure 4 except that Figure 5 is for N<sub>2</sub>O at location a and Figure 6 is for CH<sub>4</sub>. The shaded

areas on each figure are the observed range of variation of the gas concentration profiles.

Figure 7 shows the modeled RMS pressure-pumping amplitude as a function of depth through the snowpack and soil, the RMS Darcian velocity induced by the pressure gradient, and the modeled CO<sub>2</sub> drift velocity (equal to the local flux divided by the local concentration). These data correspond to 0830 LT on February 22, when the RMS pressure-pumping amplitude

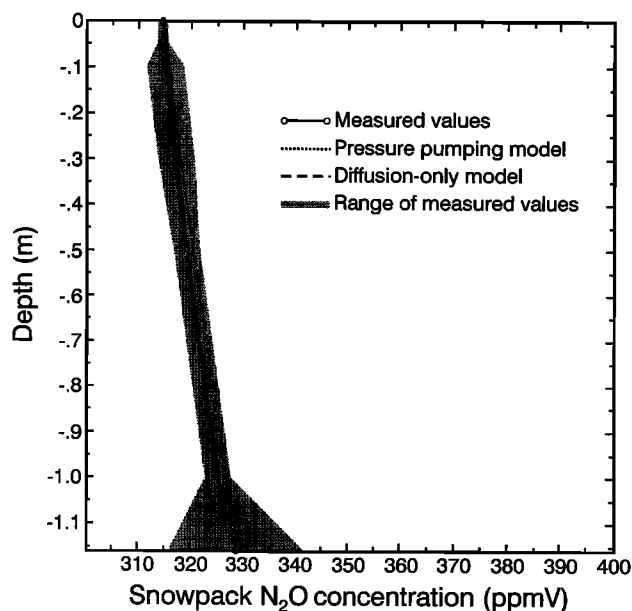


**Figure 5.** Modeled and observed snowpack N<sub>2</sub>O profiles during the experimental period February 22–24, 1995, at location “a” for the 1-D pressure-pumping model.

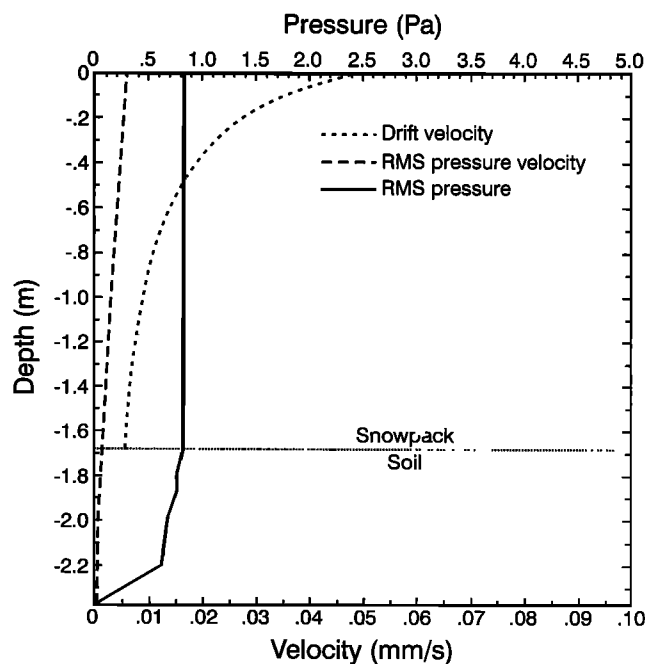


**Figure 7.** Modeled profiles of RMS pressure-pumping amplitude, the RMS Darcian advective velocity, and the drift velocity. These results are based on pressure data obtained at 0830 LT MST, February 22, 1995.

**Table 4.** Flux Estimates at Three Experimental Locations

Location (Figure 1)	CO <sub>2</sub> , mg CO <sub>2</sub> m <sup>-2</sup> s <sup>-1</sup>	N <sub>2</sub> O, ng N <sub>2</sub> O m <sup>-2</sup> s <sup>-1</sup>	CH <sub>4</sub> , ng CH <sub>4</sub> m <sup>-2</sup> s <sup>-1</sup>
<i>Diffusion-Only Model</i>			
M	0.0244	0.064	-5.80
3	0.0212	not available	-5.44
a	0.0253	0.185	-5.32
<i>Pressure-Pumping Model</i>			
M	0.0246-0.0271	0.064-0.070	-6.37 to -5.82
3	0.0213-0.0234	not available	-5.94 to -5.45
a	0.0253-0.0273	0.185-0.199	-5.66 to -5.32

Range displayed by the pressure-pumping model indicates the maximum and minimum values of the half-hourly fluxes. Maximum absolute value of the fluxes are associated with the transient caused by the initialization of the model. Minimum absolute value of the fluxes are model predictions at the end of 18 hours of simulation.

was at a minimum for phase I of the experiment. These results are quite similar to *Massman et al.* [1995] except that the RMS pressure-pumping amplitude and the RMS Darcian velocity are much less during phase I of the present study than during the period studied by *Massman et al.* [1995].

### 3.4. Flux Estimates

Table 4 is a comparison between the trace gas fluxes estimated using the diffusion-only model and the 1-D pressure-pumping model. These pressure-pumping fluxes are presented as a range of values because they include the transient associated with initialization of the model. However, after the decay of the transient, the 1-D pressure-pumping model approached a quasi-steady state that closely approximated diffusion-only flux (Figure 8). The diffusion-only solution was reached to within 3% in about 10 half hours, and the 1-D model continued to converge to the diffusion-only solution as the simulation progressed. In general, the maximum fluxes associated with the transient exceeded the diffusion-only fluxes by about 11%. Therefore the 1-D model suggests that once a quasi-steady state is reached, pressure pumping does not significantly affect simple diffusion. This conclusion differs from that of *Massman et al.* [1995], who found that turbulent atmospheric pressure pumping in the frequency range between 0.001 and 10 Hz enhances the diffusion of noninteracting trace gases through snowpacks by as much as 20% to 30%. However, the pressure-pumping simulations discussed by *Massman et al.* [1995] were not long enough to eliminate the transient. In other words, in our previous study [*Massman et al.*, 1995], we did not have enough data to fully evaluate the 1-D pressure-pumping model. To further complicate matters, the snowpack concentration profiles produced by the transient are, in general, physically realistic and quite similar to the observed profiles, so the transient cannot easily be dismissed as meaningless.

We also note here that the CO<sub>2</sub> fluxes reported by *Massman et al.* [1995] are, in general, larger than those discussed in the present study. We attribute this seasonal variation in CO<sub>2</sub> flux to the variations in soil temperature. In general, soil production rate of CO<sub>2</sub> increases with temperature [*Raich and Schlesinger*, 1992; *Peterjohn et al.*, 1994], and the soil temperatures at the meadow site were higher during the winter of 1994 ( $\approx 1^\circ\text{C}$ ) than during the 1995 winter observation period ( $\approx 0^\circ\text{C}$ ).

### 3.5. Sensitivity Analysis and Sources of Uncertainties

A sensitivity analysis is useful for evaluating the strengths and weaknesses of any modeling study. In this section we present the results of a sensitivity analysis to evaluate model uncertainties and to explore which input data and which model assumptions have the greatest influence on the flux estimates. Specifically, we calculate the change in flux estimates for changes (or uncertainties) in boundary conditions, snowpack tortuosity and density measurements, snowpack permeabilities, snowpack temperatures, soil permeabilities and temperatures, the fluctuating pressure data used to drive the model so as to include data with different amplitudes and spectral characteristics. The sensitivity analysis is also used to evaluate the importance of (1) 3-D effects and (2) the term  $(P_0/T)(\partial T/\partial t)$  discussed earlier when deriving (5).

**3.5.1. Boundary conditions, snowpack-soil characteristics and pressure.** The results of this portion of the sensitivity analysis for the 1-D model are summarized in Table 5 and are virtually identical for both the transient and the steady state solutions. None of the changes in the input parameters affected the model's tendency to converge to a diffusion-only solution. Only the results for CO<sub>2</sub> at location M (Figure 1) are reported because results from other combinations of gases and locations are similar for the 1-D model.

Table 5 indicates that the 1-D model is relatively insensitive to possible turbulent fluctuations in the upper boundary conditions for CO<sub>2</sub> but that it is sensitive to the time-invariant CO<sub>2</sub> boundary conditions. In their study of the effects of pressure pumping on snowpack temperature profiles, *Albert and McGilvary* [1992] also found that the boundary conditions play a significant role in determining the solutions to the model equations. In the present study the CO<sub>2</sub> fluxes are most sensitive to the lower boundary condition because the concentration at the soil-snowpack interface is about 8 times the ambient concentration (the upper boundary condition). The other trace gases are not necessarily so sensitive to the boundary conditions because the differences in concentration across the snowpack (lower boundary condition minus upper boundary condition)

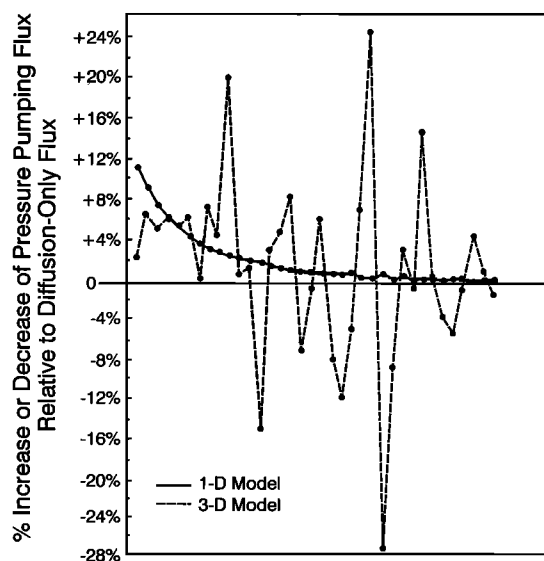


**Figure 8.** Comparison of the enhancement (or diminution) of the diffusion-only CO<sub>2</sub> fluxes for the one-dimensional and three-dimensional versions of the pressure-pumping model.

were not so large. All trace gas fluxes showed similar sensitivity to changes in snow tortuosity and snow density profiles as shown by CO<sub>2</sub>.

The fluxes are not particularly sensitive to uniform changes in snowpack permeability because changes in  $k_{\text{snow}}$  only acted to reduce the amplitude of the dynamic velocity associated with the time-varying pressure gradient but had little effect on the net dynamic flux which results from summing both the inflow and the outflow of the gas at the upper snow surface. Nor are the fluxes significantly influenced by either the soil temperatures or the snowpack temperatures, as would be expected given that the temperatures are relatively uniform and that the model equations are weak functions of temperature. Neither are the fluxes significantly influenced by the diel cycle of snowpack temperatures.

The last three tests listed in Table 5 attempt to evaluate the model's sensitivity to differences in the pressure signal used to drive the model by using three different sets of observed pressure data. These tests were performed separately on the transient and the quasi-steady state portions of the solution. To evaluate the influence of pressure amplitude on the fluxes, we used phase II pressure-pumping data, which had very similar spectral characteristics to phase I data but much larger RMS pressure amplitudes than phase I data. To investigate spectral response of the model we used the March 1994 pressure data from *Massman et al.* [1995], which showed greater power in the low frequencies, and the August–September 1993 Quad-Disc data, which showed more power in the high frequencies (Figure 3). However, because these sensitivity tests are not strictly controlled numerical tests, they can only be interpreted as suggestive or corroborative, not definitive. Nevertheless, they are useful for investigating possible model responses to other pressure signals. For the 1-D model the fluxes show virtually no sensitivity to increasing RMS pressure amplitude or to the spectral distribution of power in the pressure signal used to drive the model. These results support the previous conclusion that the diffusion is the dominant means of transfer with the 1-D pressure-pumping model.

**3.5.2. Two- and three-dimensional effects.** To test the model's sensitivity to two- and three-dimensional effects, we ran both the 1-D and the semispectral 3-D models with the same 36 contiguous half hours of pressure and input data. Figure 8 compares the pressure-pumping flux estimates (relative to the diffusion-only estimates) for both versions of the model. Two differences between the 1-D and the 3-D models are immediately apparent from this figure. First, unlike the 1-D model, the 3-D model does not display any obvious transient behavior, and second, on a half-hourly basis, two- and three-dimensional effects can enhance or diminish the diffusion-only fluxes by as much as 25%. Nevertheless, a visual inspection of the modeled CO<sub>2</sub> concentration in the snowpack during the first 3 hours of simulation did suggest the possibility of an extremely weak transient. However, the average flux during the last half of the simulation (during which the transient should further be diminished) is  $-0.3\%$  less than the diffusion-only flux, while the total ensemble averaged CO<sub>2</sub> flux (average of all 36 half hours) is only 1.5% greater than the diffusion-only flux. Consequently, we conclude that for the present 3-D simulation the transient dissipated quite quickly. Furthermore, we also conclude that on a short-term basis, two- and three-dimensional effects are important and probably should be part of any modeling study of pressure pumping. *Clarke and Waddington* [1991] demonstrated more convincingly that pressure

pumping is essentially a 3-D phenomenon. Nevertheless, the importance of long-term two- and three-dimensional effects is less obvious. For CO<sub>2</sub> they may not be important at all because a true long-term 3-D estimate of the CO<sub>2</sub> flux would be spatially averaged as well as temporally averaged, which could further smooth the deviations from the diffusion-only flux. Unfortunately, the present study was not designed to resolve questions involving estimating 3-D area-averaged fluxes. We also note here that the CO<sub>2</sub> concentration profiles simulated by the 3-D pressure pumping model were similar to the observed and 1-D model profiles shown in Figure 4, but the 3-D model CO<sub>2</sub> profiles do tend to vary more with time than the 1-D model profiles.

There are two other aspects of modeling 3-D pressure pumping that should be noted. First, the three-dimensional analytical model developed by *Clarke and Waddington* [1991] indicates that the attenuation of pressure fluctuations is much greater than predicted with the equivalent one-dimensional model. A comparison (not shown) of the pressure attenuation through the snowpack predicted by the 1-D and 3-D versions of the present numerical model displays the same quality. However, in order to insure an analytical solution to the model equations, *Clarke and Waddington* [1991] assumed that the snowpack properties were uniform with depth (i.e.,  $\rho_{\text{snow}}$  and  $k_{\text{snow}}$  are not functions of  $z$ ). However, we find that vertical layering can be important for 3-D modeling of pressure pumping in snowpacks because the terms associated with the vertical gradient of snow permeability ( $\partial k_{\text{snow}}/\partial z$ ) are often comparable in magnitude to the horizontal pressure term ( $\nabla_{\text{h}}^2 p$ ).

Second, in their study of temperature profiles in snowpacks, *Albert and MacGilvary* [1992] showed that the boundary conditions are extremely important for pressure-pumping simulations and that strong gradients can mask the effects of pressure pumping. Because the CO<sub>2</sub> gradients are much stronger than the N<sub>2</sub>O gradients, this sensitivity analysis includes the 3-D model predictions for the N<sub>2</sub>O profiles and fluxes. According to the 3-D model, the N<sub>2</sub>O fluxes can enhance the diffusion-only fluxes by several hundred percent or even completely reverse the fluxes so that they are opposite to the diffusion-only fluxes. Figure 9 compares the observed N<sub>2</sub>O profile with two profiles predicted by the 3-D pressure-pumping model. These predicted profiles correspond to a strongly enhanced flux and a reversed flux. However, these are not the most extreme examples that could have been shown because, in general, the simulated N<sub>2</sub>O profiles are quite dynamic and highly variable. Consequently, it is not possible to fully evaluate the contribution of any transient that may be present. Nevertheless, the transient is expected to be relatively minor because the CO<sub>2</sub> simulations (as discussed earlier) suggest that any transient associated with the 3-D pressure-pumping model should dissipate quickly. Unlike the 3-D CO<sub>2</sub> profiles (not shown) or the 1-D modeling results, the 3-D N<sub>2</sub>O profiles can be significantly different from the approximately linear profiles characteristic of diffusion only. However, this figure should not be taken as validating or invalidating the 3-D pressure-pumping model because these profiles correspond to just two of many profiles that are possible in what is essentially a very dynamic situation. Rather, the important conclusions here are that (1) pressure-pumping effects are more pronounced when gradients are weak, in agreement with *Albert and MacGilvary* [1992], and (2) the assumption of a constant boundary condition is likely to be incorrect for N<sub>2</sub>O. Because the observed fluctuations in ambient CO<sub>2</sub> concentration are only about 2%

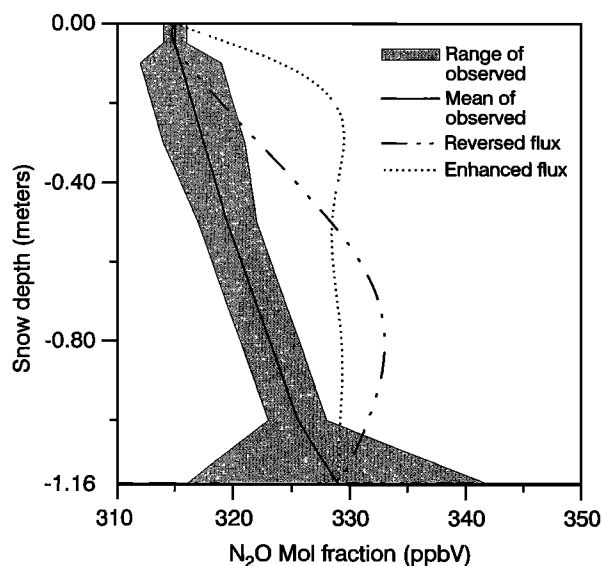


**Figure 9.** Comparison of observed snowpack  $N_2O$  profile with two  $N_2O$  profiles predicted by the 3-D model of pressure pumping at location a for February 22–24, 1995.

of the average concentration, we suspect that variations in the upper boundary condition on  $N_2O$  are also likely to be rather small. However, the 3-D model results suggest that lower boundary condition could be significantly affected. Unfortunately, at present there are no methods available for measuring high-frequency variations in  $N_2O$ , and sampling  $N_2O$  concentrations beneath the snowpack more often than once every few minutes can actually deplete the concentrations at the sampling location. However, we do note here that in general, for the three gases we have been studying, the  $N_2O$  profiles do tend to show much more variability than either  $CO_2$  or  $CH_4$  in agreement with the results of the 3-D pressure-pumping model predictions. The present  $N_2O$  results also demonstrates that some 3-D turbulent pressure-pumping effects may extend through the entire depth of the snowpack (approximately 1.7 m). In turn, this suggests that turbulent pressure-pumping effects may extend fairly deeply through soils and other porous media at the Earth's surface and that passive trace gases with weak gradients are likely to be more useful than passive tracers with strong gradients for studying the effects of pressure pumping.

Nevertheless, the  $N_2O$  results can be generalized to other gases or passive tracers. If pressure pumping is to have any significant effect on the movement of passive tracers through snowpacks, then it would have to significantly influence the boundary conditions, and the lower boundary condition is likely to be the most affected. For  $CO_2$  this means that pressure pumping (either 1-D or 3-D) is unlikely to have much effect unless the lower boundary condition is directly or indirectly influenced by pressure pumping or by some phenomenon associated with pressure pumping.

We also performed a sensitivity analysis on the 3-D pressure pumping model similar to that presented in Table 5 for the 1-D model. The half-hourly fluxes generated by the 3-D model showed greater sensitivity to changes in the time-invariant boundary conditions  $k_{snow}$ , the spectral distribution of power, and the RMS pressure amplitude than the 1-D model. However, the half-hourly fluxes showed sensitivity to the addition of

the observed fluctuations in  $CO_2$  to the upper boundary condition and to variations in  $\tau_{snow}$ ,  $\rho_{snow}$ ,  $T_{snow}$ ,  $T_{soil}$ , and the diel snowpack temperature cycle similar to that shown by the 1-D model fluxes. Although no initialization transient could be easily identified for the 3-D model, the three tests relating to spectral distribution of power and the RMS pressure amplitude were performed after an 8-hour (model time) equilibration period. These results suggest that at least in the short term, the 3-D model is much more dynamic and less dominated by diffusion than the 1-D model and that fluxes generated by 3-D models of pressure pumping are influenced by many more factors than the 1-D model. However, as was mentioned earlier, because these tests are not completely controlled numerical tests, they are not necessarily definitive, and with that caveat in mind, it is worthwhile to point out that increasing the spectral power in the high-frequency range (0.1–10 Hz) had much less influence on the fluxes than did most of the other perturbations. Within  $\pm 10\%$  and the limitations of the data the sensitivity analysis for the 3-D pressure-pumping model supports the conclusion of Albert [1993] that high-frequency pressure fluctuations do not contribute significantly to transport by pressure pumping.

**3.5.3. Turbulent fluctuations of  $(P_0/T)(\partial T/\partial t)$ .** Both the 1-D and the 3-D pressure-pumping models disregarded the temperature term  $(P_0/T)(\partial T/\partial t)$ , which, in general, tends to increase or decrease the dynamic pressure term  $\partial p/\partial t$ . On the basis of the conclusions of the above sensitivity analysis this term may not contribute much to pressure pumping unless pressure pumping is already important. However, it is useful to make an order of magnitude comparison of these two terms to estimate their relative contributions. Ignoring the time-dependent temperature term is valid if the following inequality holds:  $|\partial p/\partial t| \gg |(P_0/T)(\partial T/\partial t)|$ . Assuming that the turbulent fluctuations of  $p$  and  $T$  can be expressed as  $\exp(i\omega t)$ , where  $\omega$  is a frequency in the turbulence wave band and that

**Table 5.** Results of Model Sensitivity Analysis for  $CO_2$  Fluxes at Location M (Figure 1)

Change in Model	Relative Change $CO_2$ Flux, %
Max/min difference between upper and lower boundary conditions	$\pm 11$
Addition of turbulent $CO_2$ fluctuations observed at 1.3 m to upper boundary condition	N
$(\pm 10\%) \tau_{snow}$	$\pm 9.0$
$(\pm 10\%) \rho_{snow}$	$\mp 4.5$
$(\pm 20\%) k_{snow}$	N
$(\pm 1.5^\circ) T_{snow}$	N
$(10^{\pm 1}) k_{soil}$	N*
Uniform change in soil $T$ and change in gradient of soil $T$	N
Diel temperature cycle	N
$\pm (P_0/T)(\partial T/\partial t)$	N
Increase in RMS amplitude of $p$	N
Increase in spectral power in the 0.001–0.01 Hz band of $p$	+2†
Increase in spectral power in the 0.01–10 Hz band of $p$	+1†

N, indicates negligible change ( $<1\%$ ).

\*Massman *et al.* [1995] reported much higher sensitivities to changes in  $k_{soil}$  because of an error in the computer code. Correcting this error did not cause any significant changes in their flux estimates but did change the model sensitivity to  $k_{soil}$ .

†Maximum observed change, occurred during the transient.

the inequality holds for all frequencies within that wave band, then the above inequality reduces to  $\sigma_p \gg (P_0/T)\sigma_T$ , where  $\sigma_T$  is the RMS amplitude (square root of the variance) of the temperature fluctuations and  $\sigma_p$  is the RMS amplitude of the pressure fluctuations.

Using sonic thermometry [Kaimal and Gaynor, 1991], the observed  $\sigma_T$  during the experimental period was  $\approx 0.3^\circ\text{C}$  at 1.3 m above the surface. Because we expect  $\sigma_T$  to be less than this at the snow surface and within the snowpack, we assume that  $\sigma_T = 0.1^\circ\text{C}$  at the snow surface. Near the surface,  $T \approx 268^\circ\text{K}$  and  $P_0 \approx 70$  kPa. Therefore  $(P_0/T)\sigma_T \approx 26$  Pa, which exceeds any values of  $\sigma_p$  observed at the snow surface during the same time period. Unless  $\sigma_T$  is at least 1 or 2 orders of magnitude less than  $0.1^\circ\text{C}$ , the inequality fails at the snow surface, and ignoring the time-dependent temperature term cannot be justified on the basis of this order of magnitude evaluation. If the rates of attenuation of  $T$  and  $p$  within the snowpack are comparable, then it may not be valid to ignore  $(P_0/T)(\partial T/\partial t)$  within the snowpack either. This suggests that pressure pumping may be more appropriately described by a model that at a minimum, couples temperature and pressure. Furthermore, because the movement of water vapor can influence the temperature profiles and heat flow within the snowpack [Albert and MacGilvary, 1992], it may be necessary to include water vapor in the pressure-pumping model as well. Although the above arguments are strongly suggestive, to fully resolve the importance of the time-dependent temperature term to pressure pumping will require a model that fully couples pressure, temperature, and water vapor.

### 3.6. Possible Further Studies

First, because none of the models included soil respiration, soil uptake of  $\text{CH}_4$ , or soil nitrogen chemistry that could influence the consumption or release of  $\text{N}_2\text{O}$ , further studies of the soil processes that involve the production and consumption of these trace gases are necessary. Such studies would be useful not only in their own right but also for investigations of possible effects that pressure pumping could have on the sources and sinks of trace gases within porous media. Furthermore, if a source (sink) occurs within the snowpack (or within any porous medium), then the present study suggests that pressure-pumping effects are likely to be important if the strength of that source (sink) is influenced by pressure fluctuations or by the magnitude or direction of the associated advective velocity. Consequently, pressure pumping may significantly influence snow metamorphism because the advective effects can influence the movement of water vapor through snowpacks.

Second, the 3-D semispectral pressure-pumping model is parameterized in terms of a single horizontal wavelength primarily for illustrative purposes. A more realistic approach would include the integration over all wavelengths that could influence atmospheric pressure fluctuations. However, there are no observational or modeling studies of the composition of atmospheric pressure fluctuations by horizontal wavelength. Further studies of the effects of atmospheric pressure pumping on the exchange of mass and energy at the Earth's surface would be aided significantly by studies of the horizontal and three-dimensional structure of atmospheric pressure fluctuations.

## 4. Conclusions

The present study suggests that high-frequency turbulent pressure fluctuations in the 0.001 to 10 Hz range are unlikely to

significantly affect the rate of diffusion of passive trace gases through deep snowpacks unless the lower boundary condition (gas concentrations at the interface between the snowpack and the soil) is significantly influenced by the pressure pumping itself or by some associated phenomenon. With constant boundary conditions, simulations with the 1-D version of the pressure-pumping model indicated that (after the dissipation of the transient caused by model initialization) the effects of pressure pumping were negligible and that simple diffusion controls the transfer of  $\text{CO}_2$ ,  $\text{CH}_4$ , and  $\text{N}_2\text{O}$  through the snowpack. Furthermore, a sensitivity analysis showed that the 1-D model was sensitive only to those parameters that most strongly influence diffusion and was virtually insensitive to any parameters that influence pressure pumping. By comparing the 1-D modeling results with results from a 3-D version of the model, the sensitivity analysis also revealed the importance of two- and three-dimensional effects. The 3-D model was found to be more dynamically responsive to the influences of pressure pumping than the 1-D model. The 3-D model also predicted that for strong gradients, such as  $\text{CO}_2$ , short-term (half-hourly) fluxes were both enhanced and diminished by as much as 25% relative to the diffusion-only flux. However, when averaged over several hours, the difference between the 3-D pressure-pumping model and the diffusion-only model fluxes was only 1.5%. For weak gradients, such as  $\text{N}_2\text{O}$ , the 3-D pressure-pumping effects overwhelmed diffusion so much that the results suggested that 3-D pressure-pumping effects were quite capable of influencing the lower boundary condition.

In addition to the general conclusion above, this study suggests two other conclusions. First, an order of magnitude calculation suggests that the pressure and temperature coupling term  $((P_0/T)(\partial T/\partial t))$ , equation (4), may be quite important for studies of turbulence-driven pressure pumping. Consequently, modeling studies that include this coupling term should be performed to quantitatively assess how important it might be to pressure pumping. Unfortunately, including the coupling term adds some complexity to models of pressure pumping within snowpacks because snowpack temperature is also coupled to water vapor flow [Albert and McGilvary, 1992].

Second, the traditional basis for modeling pressure pumping, i.e., equation (5), is not valid for gases with high molecular weights or that occur in relatively high concentrations. The appendix discusses these matters in more detail. In the present study, these situations do not occur because  $\text{CO}_2$ ,  $\text{N}_2\text{O}$ , and  $\text{CH}_4$  are extremely dilute and have relatively low molecular weights.

## Appendix: Derivation of Pressure-Pumping Model From Graham's Law

The purpose of this appendix is to outline some of the approximations that are important for the development of the model equations. For the present discussion we are assuming a binary gas composed of air and some other noninteracting inert gas. The equations describing the gaseous transport of the system of gases, which are consistent with Graham's law, are developed by Farr [1993] and are given below:

$$\frac{\partial}{\partial t} (\eta c_g) = -\nabla \left( c_g v - \frac{\sqrt{M_a}}{\sqrt{M_a}\chi_a + \sqrt{M_g}\chi_g} c D_* \nabla \chi_g \right) \quad (\text{A1})$$

$$\frac{\partial}{\partial t} (\eta c_a) = -\nabla \left( c_a v - \frac{\sqrt{M_g}}{\sqrt{M_a}\chi_a + \sqrt{M_g}\chi_g} c D_* \nabla \chi_a \right) \quad (\text{A2})$$

$$\frac{\partial}{\partial t} (\eta c) = -\nabla \left( c v + \frac{\sqrt{M_g} - \sqrt{M_a}}{\sqrt{M_a} \chi_a + \sqrt{M_g} \chi_g} c D^* \nabla \chi_g \right) \quad (\text{A3})$$

where  $M_a$  is the molecular mass of air,  $M_g$  is the molecular mass of the inert gas,  $\chi_g$  and  $c_g$  are the mole fraction and the molar concentration of the inert gas,  $\chi_a$  and  $c_a$  are the mole fraction and the molar concentration of air,  $c$  is the molar concentration of the binary system (i.e.,  $c = c_g + c_a$ ), and  $D^* = \eta \tau D$ . All other symbols are the same as in the main text. We also note here that by definition,  $\chi_a + \chi_g = 1$  and that  $c_g = c \chi_g$  and that the ideal gas law can be expressed as  $c = P_0/RT$ . Strictly speaking, (A2) is not necessary for the present discussion, but it is included here for completeness. Basically, these equations are a statement of the conservation of mass for the binary system of gases. For convenience we use the three-dimensional form of the equations rather than the one-dimensional form used in the main text.

First, we assume that the porosity  $\eta$  of the medium is not changing with time, i.e., that  $\partial \eta / \partial t = 0$ . This should be valid for the snowpack during the duration of the pressure-pumping experiment. Using the steady state condition for  $\eta$  and substituting  $c_g = c \chi_g$  into (A1) yields

$$\eta c \frac{\partial \chi_g}{\partial t} + \eta \chi_g \frac{\partial c}{\partial t} = -c \nabla (\chi_g v) - \chi_g \nabla (c v) + \sqrt{M_a} \nabla \left( \frac{c D^* \nabla \chi_g}{\sqrt{M_a} \chi_a + \sqrt{M_g} \chi_g} \right) \quad (\text{A4})$$

Now multiplying (A3) by  $\chi_g$  and subtracting from (A4) and then using the identity  $\chi_a + \chi_g = 1$  yields the following advective-diffusive equation for  $\chi_g$ :

$$\eta c \frac{\partial \chi_g}{\partial t} = -c \nabla (\chi_g v) + (\sqrt{M_a} \chi_a + \sqrt{M_g} \chi_g) \nabla \left( \frac{c D^* \nabla \chi_g}{\sqrt{M_a} \chi_a + \sqrt{M_g} \chi_g} \right) \quad (\text{A5})$$

In order for (A5) to reduce to (2), two conditions must be fulfilled. These are that

$$\text{Condition A } \sqrt{M_a} \chi_a \gg \sqrt{M_g} \chi_g$$

$$\text{Condition B } \chi_a \gg \chi_g$$

We note here that if condition B is true, then  $\chi_a \approx 1$ .

For  $\text{CO}_2$ ,  $\text{N}_2\text{O}$ , and  $\text{CH}_4$  these conditions are fulfilled because, in general, their concentrations are very low (condition B) and their molecular masses are all approximately the same as  $M_a$ , which when combined with condition B insures the validity of condition A. However, (2) is not valid for gases with high molecular masses or for relatively dense gases. For example, (2) would not be valid for describing the diffusion of some organic vapors or for describing the diffusion of the binary system  $\text{N}_2/\text{O}_2$  through a snowpack or any other porous medium.

To derive (3) from (A3), we first apply conditions A and B to (A3), which yields

$$\eta \frac{\partial c}{\partial t} = -\nabla (c v) - \left( \frac{\sqrt{M_g}}{\sqrt{M_a}} - 1 \right) (\nabla (c D^* \nabla \chi_g)) \quad (\text{A6})$$

which, except for the last term on the right-hand side, is the same as (3). For (3) to be valid, therefore,  $(\sqrt{M_g}/M_a -$

$1)(\nabla (c D^* \nabla \chi_g))$  must be small compared to  $\nabla (c v)$ , which is equivalent to showing that  $|v| \gg |(\sqrt{M_g}/M_a - 1)(D^* \nabla \chi_g)|$ . The observed snowpack profiles of  $\chi_g$ ,  $\tau$ , and  $\rho_{\text{snow}}$  suggest that  $|(\sqrt{M_g}/M_a - 1)(D^* \nabla \chi_g)| \approx 4 \times 10^{-6} \text{ mm s}^{-1}$ , whereas all present results suggest that the Darcian velocity  $v$  is at least 3 orders of magnitude greater than this. Therefore if conditions A and B are fulfilled, then we can expect (3) to be a very good approximation to (A6). On the other hand, these results also indicate that in regions where the pressure gradient is very small or when the molecular mass of one gas is significantly different from air or if the diffusing gas has a high concentration relative to the carrier gas, then (3) is not valid and therefore neither is (5), which is by tradition the basis for modeling pressure pumping within porous media.

**Acknowledgments.** Our thanks to A. Bedard for his many discussions on the nature of the pressure measurements and their interpretation.

## References

- Albert, M. R., Some numerical experiments on firn ventilation with heat transfer, *Ann. Glaciol.*, 18, 161–165, 1993.
- Albert, M. R., and J. P. Hardy, Ventilation experiments in a seasonal snow cover, in *Biogeochemistry of Seasonally Snow-Covered Catchments*, edited by K. A. Tonnessen, M. W. Williams, and M. Tranter, *IAHS Publ.*, 228, 41–49, 1995.
- Albert, M. R., and W. R. McGilvary, Thermal effects due to air flow and vapor transport in dry snow, *J. Glaciol.*, 38, 273–281, 1992.
- Auble, D. L., and T. P. Meyers, An open path, fast response infrared absorption gas analyzer for  $\text{H}_2\text{O}$  and  $\text{CO}_2$ , *Boundary Layer Meteorol.*, 59, 243–256, 1992.
- Bird, R. B., W. E. Stewart, and E. N. Lightfoot, *Transport Phenomena*, John Wiley, New York, 1960.
- Bovsheverov, V. M., N. F. Gorshkov, S. O. Lomadze, and M. I. Mordukovich, Spectral characteristics of the attenuation of turbulent pressure fluctuations by spatial filtering, *Izv. Acad. Sci. USSR Atmos. Oceanic Phys.*, Engl. Transl., 9, 360–361, 1973.
- Bretznajder, S., *Prediction of Transport and Other Physical Properties of Fluids*, Pergamon, Tarrytown, N. Y., 1971.
- Clarke, G. K. C., and E. D. Waddington, A three-dimensional theory of wind pumping, *J. Glaciol.*, 37, 89–96, 1991.
- Clarke, G. K. C., D. A. Fischer, and E. D. Waddington, Wind pumping: A potential significant heat source in ice sheets, in *The Physical Basis of Ice Sheet Modeling*, edited by E. D. Waddington and J. S. Walder, *IAHS Publ.*, 170, 169–180, 1987.
- Colbeck, S. C., Air movement in snow due to wind pumping, *J. Glaciol.*, 35, 209–213, 1989.
- Colbeck, S., E. Akitaya, R. Armstrong, H. Gubler, J. Lafeuille, K. Lied, D. McClung, and E. Morris, *The International Classification for Seasonal Snow Cover on the Ground*, 23 pp., Int. Comm. on Snow and Ice, Int. Assoc. of Sci. Hydrol., Gentbrugge, Belgium, 1990. (Available from World Data Cent. for Univ. of Colo., Boulder)
- Cook, R. K., and A. J. Bedard, On the measurement of infrasound, *Geophys. J. R. Astron. Soc.*, 26, 5–11, 1971.
- Cunningham, J., and E. D. Waddington, Air flow and dry deposition of non-sea-salt sulfates in polar firn: Paleoclimate implications, *Atmos. Environ., Part A*, 27, 2943–2956, 1993.
- Farr, J. M., Advective-diffusive gaseous transport in porous media: The molecular diffusion regime, Ph.D. thesis, 133 pp., Colo. State Univ., Fort Collins, 1993.
- Gjessing, Y. T., The filtering effect of snow, in *Isotopes and Impurities in Snow and Ice Symposium*, *IASH-AISH Publ.* 118, 119–203, 1977.
- Hodgman, C. D., and N. A. Lange (Eds.), *Handbook of Chemistry and Physics*, 10th ed., CRC Press, Boca Raton, Fla., 1925.
- Houghton, J. T., G. J. Jenkins, and J. J. Ephraums (Eds.), *Climate Change, The IPCC Scientific Assessment*, Cambridge Univ. Press, New York, 1990.
- Kaimal, J. C., and J. E. Gaynor, Another look at sonic thermometry, *Boundary Layer Meteorol.*, 56, 401–410, 1991.
- List, R. J. (Ed.), *Smithsonian Meteorological Tables*, 6th rev. ed., Smithsonian Inst., Washington, D. C., 1971.

- Massmann, J., and D. F. Farrier, Effects of atmospheric pressure on gas transport in the vadose zone, *Water Resour. Res.*, **28**, 777–791, 1992.
- Massman, W., R. Sommerfeld, K. Zeller, T. Hehn, L. Hudnell, and S. Rochelle, CO<sub>2</sub> flux through a Wyoming seasonal snowpack: Diffusional and pressure pumping effects, in *Biogeochemistry of Seasonally Snow-Covered Catchments*, edited by K. A. Tonnessen, M. W. Williams, and M. Tranter, *LAHS Publ.*, **228**, 71–79, 1995.
- Mellor, M., Engineering properties of snow, *J. Glaciol.*, **19**, 15–66, 1977.
- Musselman, R. C., (Ed.), The Glacier Lakes ecosystem experiments site, *Gen. Tech. Rep. RM-249*, 94 pp., For. Serv., U.S. Dep. of Agric., Fort Collins, Colo., 1993.
- Nishiyama, R. T., and A. J. Bedard Jr., A “Quad-Disc” static pressure probe for measurement in adverse atmospheres: With a comparative review of static pressure probe designs, *Rev. Sci. Instrum.*, **62**, 2193–2204, 1991.
- Perla, R., Preparation of section planes in snow specimens, *J. Glaciol.*, **28**, 199–204, 1982.
- Peterjohn, W. T., J. M. Melillo, P. A. Steudler, K. M. Newkirk, F. P. Bowles, and J. D. Aber, Responses of trace gas fluxes and N availability to experimentally elevated soil temperatures, *Ecol. Appl.*, **4**, 617–625, 1994.
- Priestly, J. T., Correlation studies of pressure fluctuations on the ground beneath a turbulent boundary layer, *Natl. Bur. Stand. Rep. 8942*, 92 pp., Natl. Inst. of Stand. and Technol., U.S. Dep. of Comm., Gaithersburg, Md., 1965.
- Pritchard, D. T., and J. A. Currie, Diffusion coefficients of carbon dioxide, nitrous oxide, ethylene and ethane in air and their measurements, *J. Soil Sci.*, **33**, 175–184, 1982.
- Raich, J. W., and W. H. Schlesinger, The global carbon dioxide flux in soil respiration and its relationship to vegetation and climate, *Tellus, Ser. B*, **45**, 81–99, 1992.
- Roberts, R. C., Molecular diffusion of gases, in *American Institute of Physics Handbook*, 3rd ed., edited by D. E. Gray, pp. 2.249–2.252, McGraw-Hill, New York, 1972.
- Sommerfeld, R. A., and J. E. Rocchio, Permeability measurements on new and equitemperature snow, *Water Resour. Res.*, **29**, 2485–2490, 1993.
- Sommerfeld, R. A., A. R. Mosier, and R. C. Musselman, CO<sub>2</sub>, CH<sub>4</sub> and N<sub>2</sub>O flux through a Wyoming snowpack and implications for global budgets, *Nature*, **361**, 140–142, 1993.
- Sorrells, G. G., J. A. MacDonald, Z. A. Der, and E. Herrin, Earth motion caused by local atmospheric pressure changes, *Geophys. J. R. Astron. Soc.*, **26**, 83–98, 1971.
- Turco, R. P., Atmospheric chemistry, in *Climate System Modeling*, edited by K. E. Trenberth, pp. 201–240, Cambridge Univ. Press, New York, 1992.
- van Wijk, M. R., and D. A. de Vries, Periodic temperature variations in a homogeneous medium, in *Physics of Plant Environment*, edited by W. R. van Wijk, pp. 102–143, North-Holland, New York, 1963.
- Wilczak, J. M., S. P. Oncley, and A. J. Bedard Jr., Turbulent pressure fluctuations in the atmospheric surface layer, in *Tenth Symposium on Turbulence and Diffusion*, pp. 167–170, Am. Meteorol. Soc., Boston, Mass., 1992.
- Winston, G. C., B. B. Stephens, E. T. Sundquist, J. P. Hardy, and R. E. Evans, Seasonal variability in CO<sub>2</sub> transport through snow in a boreal forest, in *Biogeochemistry of Seasonally Snow-Covered Catchments*, edited by K. A. Tonnessen, M. W. Williams, and M. Tranter, *LAHS Publ.*, **228**, 61–70, 1995.
- Zimov, S. A., G. M. Zimova, S. P. Daviodov, A. I. Daviodova, Y. V. Voropaev, Z. V. Voropaeva, S. F. Prosiannikov, O. V. Prosiannikova, I. V. Semiletova, and I. P. Semiletov, Winter biotic activity and production of CO<sub>2</sub> in Siberian soils: A factor in the greenhouse effect, *J. Geophys. Res.*, **98**, 5017–5023, 1993.
- T. J. Hehn, W. J. Massman, S. G. Rochelle, R. A. Sommerfeld, and K. F. Zeller, Rocky Mountain Station, USDA Forest Service, 240 West Prospect, Fort Collins, CO 80526.  
A. R. Mosier, USDA Agricultural Research Service, P.O. Box E, Fort Collins, CO 80526.

(Received March 13, 1996; revised March 18, 1997;  
accepted March 18, 1997.)